

Compact on-chip interferometers with high spectral sensitivity

Maysamreza Chamanzar,* Babak Momeni, and Ali Adibi

School of Electrical and Computer Engineering, Georgia Institute of Technology, Atlanta, Georgia 30332, USA

*Corresponding author: chamanzar@gatech.edu

Received August 28, 2008; revised November 5, 2008; accepted November 21, 2008;
posted December 12, 2008 (Doc. ID 100748); published January 14, 2009

We introduce on-chip interferometers in which the spatial output interference pattern is observed along a detection plane. We show that by using photonic crystals with strong dispersive properties in these devices, highly sensitive interferometers can be realized. We discuss potentials of these interferometers in spectroscopy and sensing applications using their strong wavelength sensitivity and their ability to spatially map the spectral information of an input signal. © 2009 Optical Society of America

OCIS codes: 120.3180, 160.5298, 280.4788.

Implementing different optical functionalities on a chip is a crucial step for realizing integrated optical systems. Optical interferometers have conventionally been used in many applications, such as sensing, metrology, holography, and gyroscopy [1]. Conventional interferometers are usually bulky, and the interference forms in free space. The on-chip version of interferometers are primarily implemented using the Mach-Zehnder arrangement [2], in which two guided light waves interfere and the intensity of the interference at a single output port reveals the phase difference between the two arms. The dynamic range of such Mach-Zehnder interferometers is limited because of phase wrapping. This limitation is considerably alleviated if the interference pattern of the two light waves is observed along a detection plane on the chip instead of a single output port. The sensitivity of such interferometers depends on the size (or the propagation length) and the dispersive properties of the material used in their structure. Recently, efforts have been devoted to enhance the sensitivity and to minimize the size of such interferometers [3]. Particularly, it has been shown that the strong dispersion in slow-light media can be used to improve the sensitivity of these interferometers [4]. Among existing dispersive material systems, photonic crystals (PCs) exhibit interesting strong dispersive properties outside their photonic bandgap [5]. In this Letter, we show that by combining unique dispersive properties of PCs and the flexibility of observing the interference pattern on a detection plane (instead of a single output port), highly sensitive on-chip spatial interferometers can be realized, bringing about new potentials for integrated optical devices. Furthermore, these PC-based devices can be implemented using different host materials and thus are integrable in different material platforms for operation in any desired spectral range, from ultraviolet to infrared.

The structure of the proposed interferometer in the two-wave arrangement is shown in Fig. 1, which consists of a 45°-rotated square lattice PC on a silicon-on-insulator (SOI) substrate. The length of the structure in the direction of propagation is L , and its width is d . Furthermore, r is the radius of PC holes,

and a is the lattice constant. A collimated light wave illuminates the PC structure to form two refracted beams that interfere at the detection plane. The output interfaces are properly designed to convey the dispersive properties of the PC to the output wave vectors through phase matching at the interfaces. Thus, the resulting interference pattern is directly affected by the dispersive properties of the PC modes. The resulting output intensity pattern can be expressed as $I(x) = |\mathbf{E}_1 + \mathbf{E}_2|^2$, where \mathbf{E}_1 and \mathbf{E}_2 are the electric fields of the waves in the two paths. The buffer layers, indicated in Fig. 1, consist of PC layers of different lattice constant and radius designed to efficiently match the PC mode in each arm to the corresponding output fundamental diffracted-order mode and to avoid exciting higher-order diffraction modes [6].

The period of the interference pattern at the detection plane is $\Lambda = 2\pi/\Delta k_x$, in which $\Delta k_x = k_{x1} - k_{x2}$ is the difference between the two output wave-vector components along the x direction. To have a large spectral sensitivity, the PC dispersion must be engineered to maximize the variation of Δk_x with a change in the

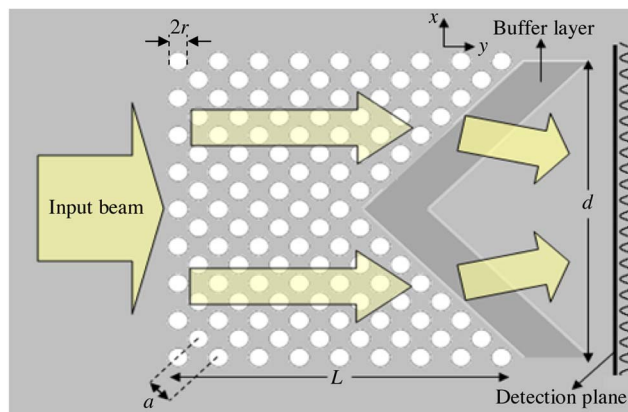


Fig. 1. (Color online) Schematic illustration of the proposed PC interferometer.

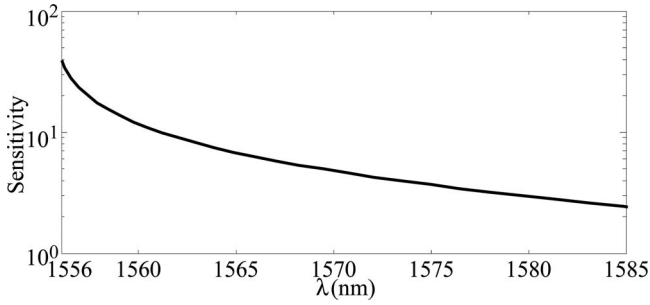


Fig. 2. Wavelength-sensitivity parameter S plotted versus wavelength for normal incidence, i.e., along the k_y direction for a 45° -rotated square lattice PC on an SOI substrate in the wavelength range where the sensitivity is large.

input wavelength. We define the wavelength sensitivity parameter S as

$$S = \left| \frac{\lambda \frac{d\Lambda}{d\lambda}}{\Lambda} \right|. \quad (1)$$

The value of S depends on the dispersion of the PC as well as the device architecture. This sensitivity parameter is defined in an ideal case, neglecting the effects such as the limited size of the structure and nonuniformity in the refracted wave amplitude. Nevertheless, S is used in the first step to obtain the appropriate operation point on the PC band structure, and later on, a cross-correlation function is defined to characterize the spectral sensitivity of the interferometer, in which the entire interference pattern is considered. To obtain the optimum operation region for any given PC structure in Fig. 1, we first calculate the PC band structure using a three-dimensional plane-wave expansion technique. Then, at each point of this band structure, we calculate S using Eq. (1) by monitoring the variation in Λ for a differential change in the operation wavelength. This procedure is carried out for a 45° -rotated square lattice slab PC on an SOI wafer (with a normalized hole radius of $r/a=0.35$, a lattice constant of $a=450$ nm, and a slab thickness of 250 nm) for TE-polarized light (with electric field in the plane of periodicity). Among the regions where S is maximum, we choose the region along the $k_x=0$ direction. In this region, S is large for a wide range of input angles, and also the design complies well with the architecture shown in Fig. 1, making the implementation of the device more practical. Figure 2 shows the variation of S with the incident wavelength in the wavelength range near the bandgap (where S is large).

One of the unique applications of the proposed PC interferometers is in spectral analysis of optical signals for spectroscopy and sensing, where the spatial-spectral mapping of the device (i.e., the output spatial intensity distributions at different wavelengths) is used to either extract the spectral content of an optical signal (in spectroscopy) or observe changes in its spectral content (in sensing). To quantify this capability of the proposed PC interferometers, we define the normalized spectral cross-correlation function as

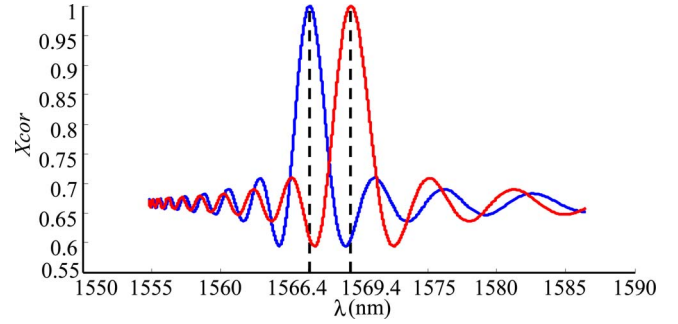


Fig. 3. (Color online) Cross correlation of the output interference patterns defined in Eq. (2) versus λ for two center wavelengths, $\lambda_0=1566.4$ nm and $\lambda_0=1569.4$ nm, obtained for the interferometer in Fig. 1 with $r/a=0.35$, $a=450$ nm, $L=50$ μm , and $d=70$ μm .

$$Xcor(\lambda_0, \lambda) = \frac{\langle I(x, \lambda_0) | I(x, \lambda) \rangle}{\sqrt{\langle I(x, \lambda_0) | I(x, \lambda_0) \rangle \langle I(x, \lambda) | I(x, \lambda) \rangle}}, \quad (2)$$

where $\langle I(x, \lambda_0) | I(x, \lambda) \rangle$ is the overlap integral of the output interference patterns at wavelengths λ_0 and λ . This cross-correlation function, $Xcor(\lambda_0, \lambda)$, is a measure of the difference between the interference patterns at wavelengths λ_0 and λ . The cross-correlation function for the PC-based interferometer in Fig. 1 (with $r/a=0.35$, $a=450$ nm, $L=50$ μm , and $d=70$ μm) is plotted in Fig. 3 (for a TE-polarized incident beam, at the optimum operation range shown in Fig. 2) as a function of wavelength (λ) for two different values of the center wavelength ($\lambda_0 = 1566.4$ nm and $\lambda_0 = 1569.4$ nm). It can be seen that these two wavelengths (which are just 3 nm apart) can be well distinguished using the cross-correlation function peaks. Some practical issues have been considered for obtaining these results. For example, the period of the output interference pattern should be large enough to be properly detected. We use the FWHM of the cross-correlation function as the spectral resolving performance measure. Devices with smaller FWHM of $Xcor(\lambda_0, \lambda)$ can distinguish smaller spectral features (i.e., better spectral resolution). This FWHM is plotted in Fig. 4 for the proposed interferometer in a range of 30 nm bandwidth. Also plotted in this figure is the FWHM for the interferometer without PC, in which the two waves propa-

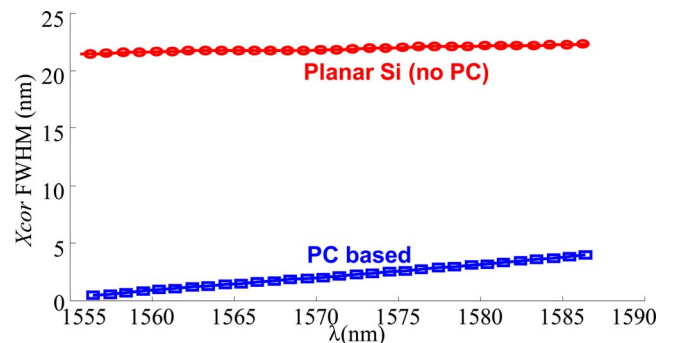


Fig. 4. (Color online) FWHM of the cross-correlation function versus λ for the interferometer in Fig. 1 with PC (squares), and with planar Si and no PC (circles).

gate in the background material (i.e., an Si slab). It can be seen that the PC-based interferometer has a cross-correlation FWHM of more than 1 order of magnitude smaller, indicating more than 1 order of magnitude higher resolution.

The proposed on-chip interferometer can also be used to detect phase difference between its two arms when excited by a monochromatic input light wave and thus can have applications as a sensor in lab-on-a-chip sensing systems. In this regard, one arm of the interferometer in Fig. 1 can be used as the interaction region where the specimen to be sensed infiltrates the PC holes and/or covers the top of the structure. In this configuration, the average refractive index is changed in one arm of the interferometer, causing a phase difference between the two arms and thus a corresponding change in the output interference pattern.

The overall performance of the proposed on-chip PC-based spatial interferometer depends on the dispersion of the PC as well as the architecture of the device. For the specific architecture given in Fig. 1, the optimum operation region on the PC band structure is found by an exhaustive search over the first band of the band structure of a square lattice PC; potentials still remain to be investigated for higher photonic bands or other PC lattices. The width of the structure (d , as shown in Fig. 1) also affects the sensitivity of the interferometer directly; i.e., the larger the width (d), the smaller the FWHM of X_{cor} . The length of the structure, L , is related to d through the angle of the output interfaces (45° in our design). By using strongly dispersive PCs, the size of the structure can be minimized for a required resolution. In particular, the interferometer presented in this work has an overall size of $50 \mu\text{m} \times 70 \mu\text{m}$ for operation around 1560 nm. The architecture is a close-to-optimal functional option; nevertheless, there might be more efficient configurations, depending on the application. The dispersion of the PC varies non-uniformly with the frequency, thus limiting the operation bandwidth of the device. Increasing the bandwidth with a specific PC (working at its optimal operation point) deteriorates the resolution, which in turn can be compensated by increasing the size of the structure. Therefore, a compromise should be met for the operation bandwidth, the device size, and the spectral resolution.

Some issues need to be considered for practical implementation of the proposed interferometers, including input/output coupling, insertion loss, and propagation loss. Inappropriate input/output coupling adversely affects the performance of the interferometer by reducing the throughput or by exciting undesired modes appearing at the output as unwanted interfering signals. To avoid undesired modes, an on-chip collimating mirror can be used at the input interface to form a collimated incident light wave, which guarantees the excitation of the desired

PC mode at each wavelength and minimizes the input spatial harmonic spread. Adiabatic matching layers [7] may be used for reducing the insertion loss. For example, in the presented particular design the insertion loss is better than 3 dB over the operation bandwidth without any matching layers, which can be significantly reduced by using appropriate matching layers. Output buffer layers [6], as described earlier, can be used so that the coupling efficiency to the desired output diffraction order is maximized and other higher diffraction orders are not excited. Propagation loss that reduces the output signal-to-noise ratio and causes nonuniformity in the amplitude of the output refracted waves and correspondingly degrades the fringe visibility is primarily caused by fabrication imperfections that are nowadays considerably alleviated as a result of ongoing efforts on improving the quality of fabrication [8]. Small deviations in the PC hole sizes may occur in fabrication; fortunately, this does not significantly affect the performance, as it occurs evenly in both arms and will be accounted for in the calibration process for spectrometer application. The temperature-dependent change of refractive index also occurs evenly in both arms as well as the input and output regions and has a minimal effect on the performance of the device.

In conclusion, we showed that using PCs makes it possible to form compact, on-chip, and highly sensitive spatial interferometers in which the interference pattern is observed along a detection plane. We showed that by using PCs the wavelength sensitivity and resolution of such interferometers are considerably improved compared to conventional interferometers. The large spectral sensitivity of these interferometers (caused by the strong PC dispersion) and the spatial mapping of the spectral information in the output plane make these interferometers interesting choices for spectroscopy and sensing applications.

This work has been supported by the National Science Foundation (NSF), contract ECCS-0742063, and by the Air Force Office of Scientific Research (AFOSR), grant FA9550-07-1-0201 (G. Pomrenke).

References

1. P. Hariharan, *Optical Interferometry* (Academic, 2003).
2. M. Lipson, *J. Lightwave Technol.* **23**, 4222 (2005).
3. E. A. Camargo, H. M. H. Chong, and R. M. De La Rue, *Appl. Opt.* **45**, 6507 (2006).
4. Z. Shi, R. Boyd, D. Gauthier, and C. Dudley, *Opt. Lett.* **32**, 915 (2007).
5. B. Momeni and A. Adibi, *J. Lightwave Technol.* **23**, 1522 (2005).
6. B. Momeni, M. Chamanzar, E. Shah Hosseini, M. Soltani, M. Askari, and A. Adibi, *Opt. Express* **16**, 14213 (2008).
7. B. Momeni and A. Adibi, *Appl. Phys. Lett.* **87**, 171104 (2005).
8. M. Soltani, S. Yegnanarayanan, and A. Adibi, *Opt. Express* **15**, 4694 (2007).